

Design and Simulation of a Micromachined Accelerometer

HAZEM HASSAN*, HASSAN IBRAHIM**, and SALAH ELSEDAWY***

Electronics and Communication Engineering
 Arab Academy for Science and Technology and Maritime Transport
 EGYPT

Abstract: - The model parameters of the micromachined tunnelling accelerometer have a significant effect on the accelerometer’s performance, including its range, bandwidth, sensitivity, accuracy and even the interfacing circuitry. This paper presents the design, simulation and development of a low voltage micromachined tunnelling microaccelerometer and the effects of parameter on the accelerometer’s performance. The derivation of the sensing accelerometer model will be discussed. With the use of the MATLAB simulation program, the real world effects of the various parameters are revealed.

Keywords: - MEMS tunnelling accelerometer, Electrostatic, Sensing, Sensitivity, Low spring constant

1. Introduction

Since the development of micro-electro-mechanical system (MEMS) inertial instruments have undergone significant progress over the last few decades. The significant advantages of low cost, low power, compact size and batch fabrication allows MEMS based inertial sensors to serve a wide range of applications, as demonstrated in table 1. As can be seen from the table 1 the typical performance requirements for each application are considerably different.

Recently, a new class of micro machined sensors has appeared that makes use of a constant tunnelling current between one tunnelling tip (attached to a movable macrostructure) and its counter electrode to sense deflection. This is viable due to the exponential relationship of the tunnelling distance with the tunnelling current [1].

A low voltage operation (approximately 5-15V) is vital if micro machined tunnelling sensors are to find widespread success in commercial application. In particular, this low voltage allows the readout electronics of tunnelling devices to be complementary metal-oxide semiconductor CMOS compatible, thus enabling them to be incorporated into a portable battery – operated by multi sensors instrumentation Microsystems [1].

Application	Bandwidth	Resolution
Automotive		
Airbag release	0-0.5 kHz	<500 mG
Stability and active control systems	0-0.5 kHz	<10 mG
	dc-1kHz	<10 mG
Active suspension		
Inertial navigation	0-100Hz	<5µG
Seismic activity		
Shipping of fragile Goods	0-1 kHz	<100mG
Space Microgravity Measurements	0-10Hz	<1µG
Medical Applications	0-100Hz	<10mG
Vibration Monitoring	1-100KHz	<100mG
Virtual reality (head-mounted displays and data gloves)	0-100Hz	<1mG
Smart ammunition	10Hz-100KHz	1G

Table 1. Typical performance requirements for each application for each application [2].

2. Device structure and operation Principle

Figure 1 shows the device’s cross-section. The device incorporates two levels of silicon and one of glass. The first level of silicon contains one proof mass with the tunnelling tip, and cantilever beams anchored to the glass substrate. The second silicon is the fixed microstructure that acts as the top deflection electrode. The glass substrate supports the first and second silicon microstructure and two metal electrodes, one of which is the tunnelling counter electrode and the other is the bottom deflection electrode [3][4].

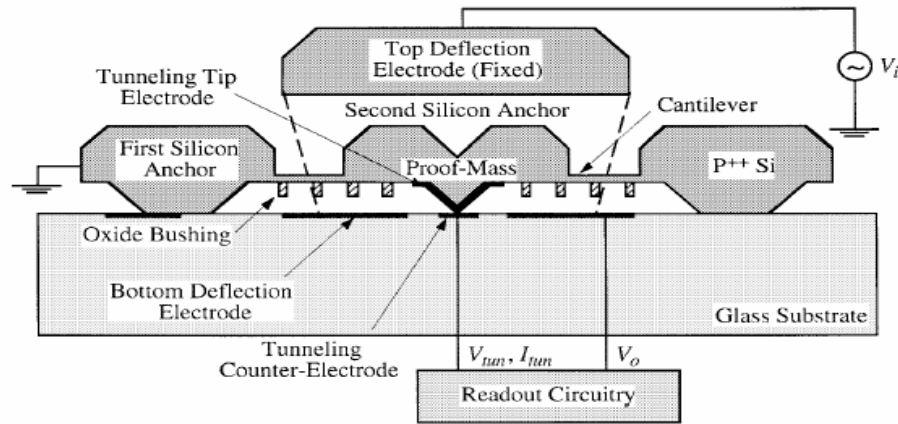


Fig.1 Cross section of a low voltage tunneling based silicon micro-accelerometer

The operation principle for tunnelling based microsensors is simple. As the tip is brought sufficiently close to the counter electrode (approximately 10V), using electrostatic force generated by the bottom deflection electrode, a tunnelling current is established. This remains constant if the tunnelling voltage and the tunnelling distance between the two electrodes remain unchanged. Once the proof mass is displaced due to acceleration, a readout circuit responds to the change of the tunnelling current and adjusts the bottom deflection voltage to move the proof mass back, thus maintaining a constant tunnelling current [3][4].

Hence acceleration can be measured by reading out the bottom deflection voltage. The top deflection electrode is used to simulate acceleration electrostatically for self test and to protect against over range [7]

The relation between the tunnelling current I_{tun} and the displacement Δx at low tunnelling voltage is

$$I_{tun} \propto V_{tun} \exp(-\alpha x \sqrt{\phi}) \quad (1)$$

$$\frac{\Delta I_{tun}}{\Delta x} = I_{tun} \cdot \alpha \sqrt{\phi} \quad (2)$$

Where v_{tun} is the tunnelling voltage, x is the tunnelling distance, α is a constant $1.025 \text{ A}^{-1} \text{ eV}^{-1/2}$, and Φ is the height of the tunnelling barrier. In a pair

of parallel plates (the proof mass and the bottom deflection electrode), the electrostatic feedback force F_{eq} , generated by the bottom deflection voltage V_o , is:

$$F_{eq} = \frac{\epsilon_o A_b V_o^2}{2h_b^2} = k \Delta x \quad (3)$$

Where ϵ_o is the permittivity in air, A_o is the plate area, and h_b is the distance between the proof mass and the bottom electrode

For optimum performance, tunnelling based micro-accelerometers need to be operated in a closed loop mode [3], [4]. The reasons are as follows: Firstly, the ratio of the change in the tunneling current to the change in the tunneling distance is extremely large, thus limiting their measurement range if they are operated in an open loop mode. Secondly, the tunneling barrier height for two tunneling electrodes may vary by one order of magnitude in air [3], [5], thus affecting open loop device sensitivity directly. This is undesirable in closed loop operation the movable structure are virtually stationary so that a large distance to current gain does not limit the measurement range of tunnelling based devices. Furthermore, closed loop devices sensitivity is determined only by the electrostatic feedback force rather than the tunnelling barrier height [3] [4].

3. Analyses and mathematical model

As shown in Figure 2 the block diagram of the closed loop system for a low voltage tunneling based microaccelerometer presented in [1] consists of four subsystems, suspended proof mass; tunneling based mechanism, current to voltage amplifier, and electrostatic feedback, the overall mathematical model can be developed as follows

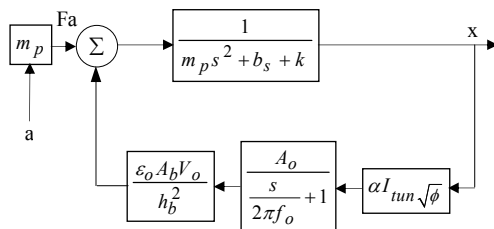


Fig.2 block diagram for overall system

The proof mass is developed as mechanical system represented by a mass (m_p), spring constant (k) and damping coefficient (b). The initial force f_a is transferred due to the acceleration (a), input to the system, into the displacement of the proof mass x with respect to the system frame. The mathematical equation for the mass can be developed using Newton equation for motion, in s domain as follows

$$F_{applied} = F_a - F_{elect} = (m_p s^2 + b_s + k)x \tag{4}$$

Where $F_{applied}$ is the applied force, the resultant between the external system input force and the accelerometer internal electrostatic force, F_a is the system input force, where $F_a = a * m_p$, a is the system acceleration, F_{elec} microaccelerometer electrostatic force comes from the feedback, x is the proof mass displacement

The transfer function of the proof mass can be found as follows

$$G_1 = \frac{x}{F_{applied}} = \frac{1}{m_p s^2 + b_s + k} \tag{5}$$

The displacement of the proof mass with respect to the system frame induces a change in the tunneling

Current I_{tun} . This current flows in the circuit of the fixed electrode. The relation between the mass displacement and this tunneling current is nonlinear. Displacement is proportionally increases with the tunneling current as represented in equation (6)

$$I_{tun} \propto e^{\sqrt{x}} \tag{6}$$

The constant of proportionality can be defined as shown in equation (7)

$$I_{tun} = I_0 \alpha e^{-\alpha \sqrt{\phi x}} \tag{7}$$

Where Φ is the tunneling barrier height for two tunneling electrode. I_0 is the initial tunneling current when the gap between the moving mass and the bottom electrode is x .

at the current to voltage block the input signal is essentially a current, and thus the signal source is most conveniently represented by its Norton equivalent. The output quantity of interest is volt. The volte signal can be taken across resistance at the output terminal. Fig (3) shows the model for such amplifier [6], which can be implemented using BJT or JFET transistors R_i , R_o is the amplifier input and output resistance, A_i is the amplifier gain as in equation (8). The current to voltage amplifier has a dc gain A_o defined as in equation (8)

$$A_i = \frac{i_o}{i_i} \quad A_o = \frac{i_o}{i_i} \Big|_{V_o=0} \tag{8}$$

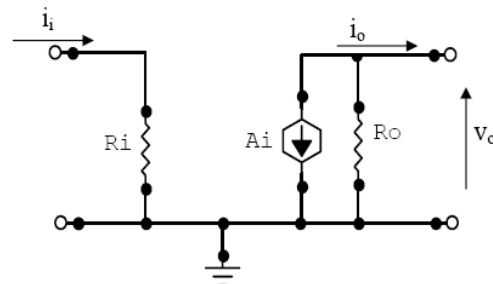


Fig.3 current to voltage amplifier model

Where i_o the amplifier output is current, i_i is the amplifier input current and v_o is the amplifier output voltage in the time domain. The current to voltage amplifier transfer function (s domain) is represented by the relation between the input signal (tunneling current I_{tun}) and the output signal (output voltage v_o). The amplifier transfer function is shown in equation (9). It works as low pass filter system. Where it is a first order system with only one dominant pole at $2\pi f_o$

$$G_2 = \frac{V_o}{I_{tun}} = \frac{A_o}{1 + \frac{s}{2\pi f_o}} \tag{9}$$

Where f_o is the break frequency in Hz, it is the cut off frequency for the current to voltage amplifier (-3db frequency on the current to voltage bode plot graph).

The feedback system works using the electrostatic actuation technique to bring the proof mass back to its original position. The applied voltage on two conducting plates generates electrostatic force; this force may be attractive or repulsive according to the charge type (positive or negative) on each plate. In general, in the time domain, the electrostatic force can be represented as in equation (10)

$$f_{ele} = \frac{1}{2} \times \frac{\epsilon A}{x_o^2} \times v^2 \tag{10}$$

Where v is applied voltage on the plates, $\epsilon = \epsilon_o$ (permittivity of the free space 8.85×10^{-12}) where the media between two electrodes is the air, A is the plate area and x_o is the gap between the plates. Finally, in our case, in the s domain, the output voltage signal v_o generates and controls the electrostatic force, on the form of equation (10), F_{elect} to bring the proof mass back to its original position by means of negative feedback. Where this electrostatic force represented in equation (11) proportionally increases with A_b (the electrode area). Decrease with squaring of h_b (the distance between the proof mass and bottom deflection electrode)

$$F_{elect} = \frac{\epsilon_o A_b V_o}{h_b^2} \tag{11}$$

The above subsystems can be summarized as in fig (2). The transfer function of the closed loop sensors system can be expressed as in equation (12)

$$G(s) = \frac{x(s)}{a(s)} = \frac{x}{1 + x * \alpha I_{tun} \sqrt{\phi} * y * z} \tag{12}$$

Where

$$x = \frac{1}{m p s^2 + b s + k} \quad y = \frac{A_o}{(\frac{s}{2\pi f_o} + 1)}$$

$$z = \frac{\epsilon_o A b v_o}{h p^2}$$

Let

$$K_T = \alpha I_{tun} \sqrt{\phi} \quad K_{FB} = \frac{\epsilon_o A_b V_o}{h_b^2} \quad \omega_o = 2\pi f_o$$

Then

$$G(s) = \frac{X(s)}{a(s)} = \frac{\frac{s}{\omega_o} + 1}{x_1 s^3 + y_1 s^2 + z_1 s + k + K_T K_{FB} A_o} \tag{13}$$

Where

$$x_1 = \frac{m p}{\omega_o} \quad y_1 = (m_p + \frac{b}{\omega_o})$$

$$z_1 = (b + \frac{k}{\omega_o})$$

Sensitivity and bandwidth are the two main design parameters for accelerometer. The accelerometer sensitivity can be expressed as follows [1]

$$s_o = \rho_p t_p h_b \sqrt{\frac{A_b}{2 \epsilon_o k x_o}} \tag{14}$$

Where ρ_p and t_p are the material density and thickness of the proof mass, respectively, and x_o is the initial distance between the two tunneling electrode. And it is assumed that the proof mass and bottom deflection electrode have the same area A_b . It is found that the easiest method to scale the sensitivity is to change the thickness of the proof mass since the martial density of the proof mass is a constant for a given martial and a change of the other design parameters varies the output offset voltage, according to the equation above (14), a number of conclusions can be drawn as follows:-

1- Device sensitivity is linearly proportional to the proof mass thickness as well as the square root of the proof mass area as shown in fig (5). However, a large increase in the proof mass would significantly reduce the bandwidth of the closed loop system [1], figure (4) shows the bandwidth versus different mass dimensions.

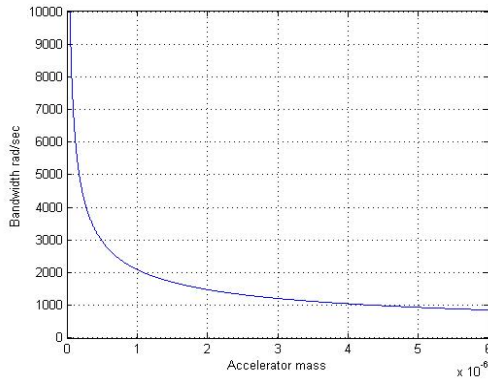


Fig.4 Bandwidth vs. accelerometer mass

2- Device sensitivity is inversely proportional to the square root of the spring constant, while the bandwidth of the closed loop system increases with spring constant [1].

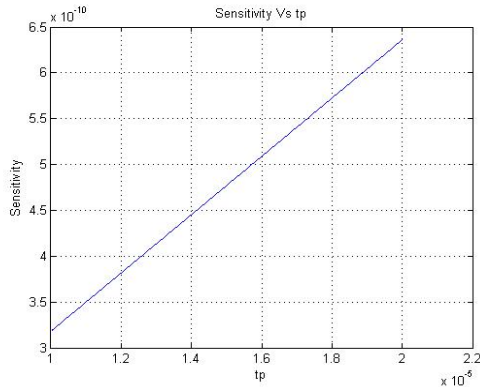


Fig.5 sensitivity vs. proof mass thickness

3- Device sensitivity does not affect by squeeze film damping coefficient, but at the same time a very large squeeze film damping coefficient reduces the bandwidth of the closed loop system while a very small damping coefficient may cause the closed loop system to become unstable [1].

4-an increase in the bandwidth of the current-to-voltage amplifier does not affect the accelerometer sensitivity, where it increase the bandwidth of the closed loop system significantly (it brings the system from an over damped to under damped state). From the root locus analysis fig (6, 9, 10) one can find that. Fig (9) shows the closed loop frequency response, for

50 KHz bandwidth current to voltage amplifier, the closed loop system bandwidth is about 28 KHz. And when the current to voltage amplifier bandwidth has been reduced to 1 Hz, the closed loop system bandwidth becomes 100 KHz as shown in fig (10).

4. Experimental results

Table (2) presents the nominal design parameters used in this design for the accelerometer taken from [1] the design value of the sensitivity for the accelerometer presented in [1][4] is 161 mV/g and the sensitivity is scaled by changing the thickness of the proof mass where the material density of the proof mass is a constant for a given material, and the change of the other design parameters varies the output offset voltage.

Nominal design parameters	values
m_p	5.576 μ
k	4.42 N/M
b	1.097*10 ⁻³ N.S/M (air)
f_0	5 KHz
$\frac{K_T A_0 K_{FB}}{K}$	5
$K_T A_0 K_{FB}$	22.1 N/M

Table 2 nominal design parameters for the accelerometer

Intensive simulation has been done using MATLAB, the results obtained from the simulation are declared as follows. The system has three poles at (-31542 -35 +2176i -35 -2176i), and a zero at -3154, they are all in the left hand side in the complex plan, which assures the system stability. From the impulse response for the accelerometer system one can find that, the system response reaches zero at time 0.18 sec.

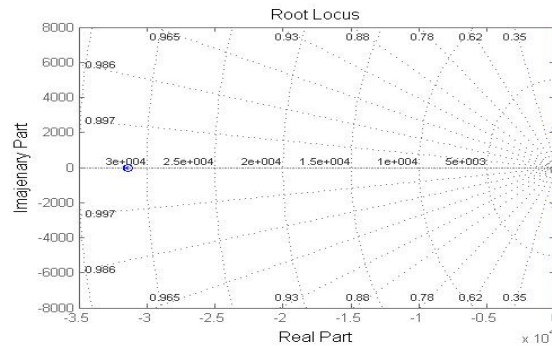


Fig.6 root locus for closed loop system

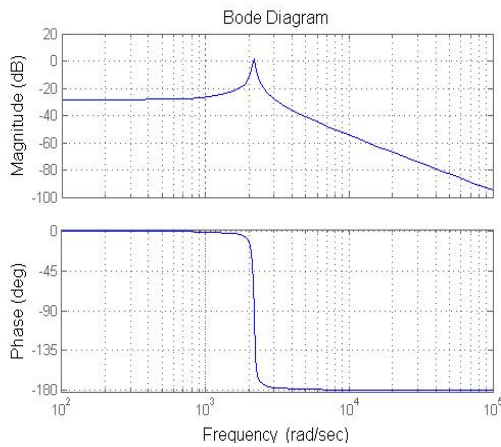


Fig.7 magnitude and angel bode plot for closed loop system

Fig (6) (7) show the root locus and bode plot for the accelerometer closed loop system. The frequency response of the closed loop system can be computed from the transfer function by replacing s by $j\omega$. One can note that, as the loop gain $\frac{K_T A_o K_{FB}}{K}$ increases as the system poles move on the root locus and the frequency response amplitude increases and goes to positive value. Fig (8) shows the step response for the system, it reaches 4% from the reference value at steady state, which means 96% error. The step input here represents the system acceleration input (to be sensed) and the system output is the mass displacement, which will be measured, by means of the variations in the tunnelling current, to give the accelerometer sensors reading.

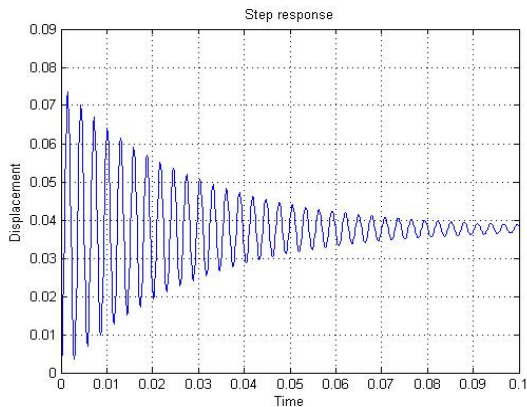


Fig.8 system step response

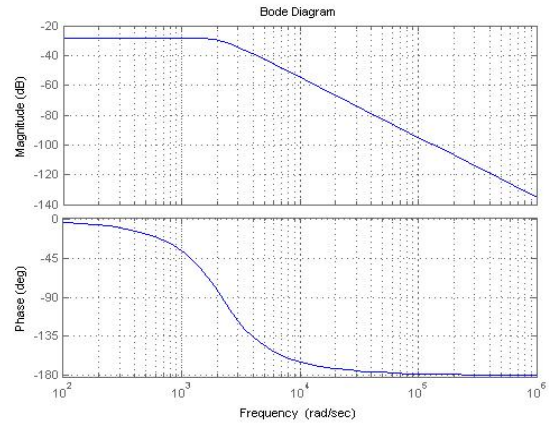


Fig.9 closed loop system bode plot using current to voltage amplifier bandwidth at 50 KHz

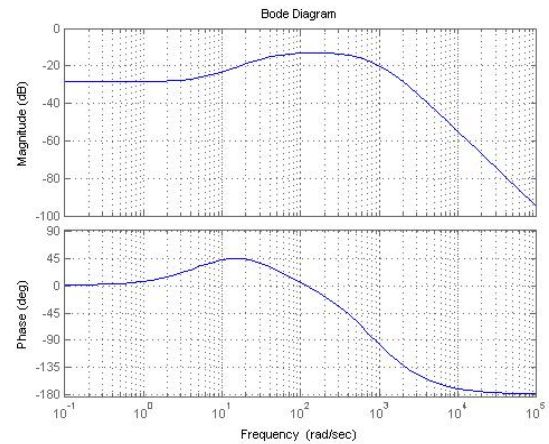


Fig.10 closed loop system bode plot using current to voltage amplifier bandwidth at 1 Hz

5. Conclusions

Microaccelerometer analysis has been presented with optimization objective in mind. Microaccelerometer model is presented and simulated using MATLAB. Device sensitivity, bandwidth for the microaccelerometer closed loop system are investigated. The simulation gave us conclusion that, the closed loop system parameters mass m_p , spring constant k , damping ratio b and closed loop gain k_c have big effect on increasing and decreasing the system bandwidth, accuracy, system type (damping and over damping) and system time response.

References

- [1] Chingwen Yeh and Khalil Najafi, “*CMOS Interface Circuitry for a Low-voltage Micromachined Tunneling Accelerometer*”, Journal Of Microelectromechanical System, vol. 7, No. 1, MARCH 1998.
- [2] S. Beeby, G. Ensell, M. Kraft, N. White, “MEMS Mechanical Sensors” pp. 175-190.
- [3] Chingwen Yeh and Khalil Najafi, “A Low Voltage tunnelling-Based silicon microaccelerometer”.
- [4] Chingwen Yeh and Khalil Najafi, “A Low Voltage bulk-silicon tunnelling-Based microaccelerometer”
- [5] T.W. Kenny et al., “widewidth electromechanical actuators for tunneling displacement transducer,” IEEE J.microelectromech. sys. St., vol. 3, NO. 3, pp. 97-104, 1994.
- [6] A.S. Sedra, K. C. Smith, “microelectronic circuits”, New York, Oxford, 1998.